



## Current cross correlations in a quantum Hall collider at filling factor two

Edvin G. Idrisov <sup>1</sup>, Ivan P. Levkivskiy <sup>2</sup>, Eugene V. Sukhorukov,<sup>3</sup> and Thomas L. Schmidt<sup>1</sup>

<sup>1</sup>*Department of Physics and Materials Science, University of Luxembourg, L-1511 Luxembourg, Luxembourg*

<sup>2</sup>*Dropbox Ireland, One Park Place, Hatch Street Upper, Dublin, Ireland*

<sup>3</sup>*Département de Physique Théorique, Université de Genève, CH-1211 Genève 4, Switzerland*



(Received 8 February 2022; revised 4 July 2022; accepted 12 July 2022; published 3 August 2022)

We use the nonequilibrium bosonization technique to study the effects of Coulomb interactions in mesoscopic electron colliders based on quantum Hall edge states at filling factor  $\nu = 2$ . The current cross correlations and Fano factor, which carry the information about the exclusion statistics, are calculated. It is shown that both these quantities have a nonanalytical dependence on the source transparency, which scales as  $\log(1/T_s)$  at small  $T_s \ll 1$ . This is a consequence of electron-electron interactions in the outgoing nonequilibrium states of the collider.

DOI: [10.1103/PhysRevB.106.085405](https://doi.org/10.1103/PhysRevB.106.085405)

### I. INTRODUCTION

The progress in experimental techniques at the nanoscale has allowed experimentalists to design composite systems based on quantum Hall (QH) edge states [1–4]. This development has already led to a better understanding of fundamental phenomena in mesoscopic physics, such as phase coherence [5–11], charge and heat quantization [12–18], as well as equilibration and relaxation [19–28]. In particular, these novel architectures have started the field of electron quantum optics, where devices and phenomena known from optics have been recreated in the electronic domain.

One essential element of these experimental setups is a quantum point contact (QPC), i.e., a narrow channel between two electrically conducting systems [29]. In the context of electron quantum optics, such QPCs act as electron beam splitters and provide a platform for tunneling experiments in the presence of different kinds of injection sources [30–33]. Particular examples are electron analogs of the photonic Hong-Ou-Mandel, Hanbury Brown and Twiss, Mach-Zehnder, and Fabry-Pérot experiments [34]. The current and shot noise through a QPC connecting integer and fractional QH edge states have been measured in several experiments [2]. These studies have made it possible to distinguish Fermi-liquid and non-Fermi-liquid phases in current-voltage characteristics and in the corresponding current noise [35–45]. Apart from that, it is worth mentioning that the noise provides one of the most straightforward methods to measure the effective charge of tunneling quasiparticles in the fractional QH regime [46].

Using a combination of QPCs, experimentalists were able recently to build anyonic colliders at a fractional filling factor  $\nu = 1/m$  (where  $m$  is an odd integer) and integer filling factor  $\nu = 2$  [47]. Their measurements of the current cross correlations at zero frequency and the generalized Fano factor have provided evidence for anyonic exclusion statistics of charge carriers. This agrees with the theoretical predictions for the Laughlin state at  $\nu = 1/3$  [48]. It is worth mentioning that

for conventional Mach-Zehnder and Fabry-Pérot interferometers, the measured current or conductance is sensitive to the exchange statistics [49]. The latter is not necessarily related to the exclusion statistics. For instance, interacting bosons with strong delta-functional repulsion have the same exclusion statistics as fermions, however, their exchange statistics are different.

In this paper, we consider a mesoscopic electron collider based on QH edge states at integer filling factor  $\nu = 2$ , where the incoming nonequilibrium states are created using two quantum point contacts (QPC1 and QPC2), with respective transparencies  $T_{1s} \ll 1$ , where  $s \in \{u, d\}$  denotes the upper and lower channels (see Fig. 1 for a schematic illustration). At zero temperature, the resulting incoming states have “double-step” distribution functions  $f_{1s}(\epsilon) = \theta(-\epsilon) + T_{1s}\theta(\epsilon)\theta(V - \epsilon)$ , where  $V$  is the source voltage. Due to Coulomb interactions the incoming states split into two modes with different velocities. Subsequently, the nonequilibrium modes arriving from the upper and lower part of the collider are mixed by a third QPC (QPC3) with transparency  $T$ . In order to investigate the statistical fluctuations after the collision at QPC3, which yield information about the exclusion statistics, we calculate the zero-frequency cross correlations of the current [47]

$$S_{1u;1d}(\omega = 0) = 2 \int dt \langle \delta j_{1u}(t) \delta j_{1d}(0) \rangle, \quad (1)$$

where  $\delta j_{1s}(t) = j_{1s}(t) - \langle j_{1s}(t) \rangle$  and the average is taken with respect to the nonequilibrium state created by injection currents from QPC1 and QPC2. This quantity has been measured in a recent experiment [47]. For chiral fermions the current in Eq. (1) is proportional to the charge density,  $j_{1s}(x, t) \propto \psi_{1s}^\dagger(x, t)\psi_{1s}(x, t)$ . Apart from the current noise, we are interested in the generalized Fano factor, which contains information about the exclusion statistics [47]. It is defined as

$$P = \frac{S_{1u;1d}(0)}{2eT(1-T)I_+}, \quad (2)$$

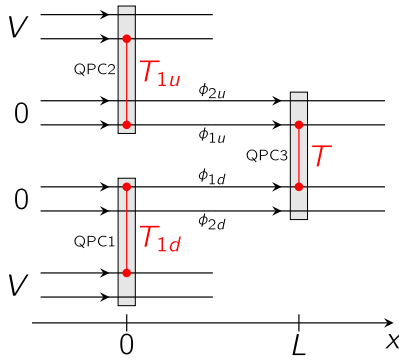


FIG. 1. Schematic picture of a mesoscopic electron collider based on QH edge states at filling factor  $\nu = 2$ . Two independent voltage-biased sources QPC1 and QPC2 with respective transparencies  $T_{1d}$  and  $T_{1u}$  generate nonequilibrium states at the upper and lower edges, which collide at QPC3 with transparency  $T$ . The zero-frequency current noise  $j_{1u}(t)$  and  $j_{1d}(t)$  after QPC3 is measured. The charge density fields are expressed in terms of nonequilibrium chiral boson fields  $\phi_{\alpha s}(x, t)$ , where  $\alpha \in \{1, 2\}$  and  $s \in \{u, d\}$ .

where  $I_+ = e^2 V (T_{1u} + T_{1d}) / 2\pi \hbar$  is the total input current. The theoretical study of current cross correlations is non-trivial since one has to deal with a nonequilibrium situation due to the injection QPCs as well as with strong electron-electron interactions. For this reason, it is convenient to use the nonequilibrium bosonization approach [50–53] which we explain below. Throughout the paper, we focus on the case of zero temperature. We set  $|e| = \hbar = k_B = 1$  during the calculation and restore the dimensions in the main results for the noise at the end.

## II. THEORETICAL METHOD

To study quantum Hall edge states at filling factor  $\nu = 2$ , it is convenient to use their effective field theory [54]. According to this, the low-energy degrees of freedom of the edge states are collective fluctuations of the charge densities  $\rho_{\alpha s}(x)$ , where the subscripts  $\alpha \in \{1, 2\}$  and  $s \in \{u, d\}$  denote the channels (see Fig. 1). The fermionic fields  $\psi_{\alpha s}(x, t) \propto \exp[i\phi_{\alpha s}(x, t)]$  and the charge density fields,  $\rho_{\alpha s}(x, t) = (1/2\pi)\partial_x \phi_{\alpha s}(x, t)$ , are represented in terms of chiral boson fields which satisfy the standard equal-time commutation relations

$$[\phi_{\alpha s}(x, t), \phi_{\beta r}(y, t)] = i\pi \delta_{\alpha\beta} \delta_{sr} \operatorname{sgn}(x - y). \quad (3)$$

The Hamiltonian of the edge states in the presence of Coulomb interactions is given by

$$H = \frac{1}{2} \sum_{s, \alpha\beta} \iint dx dy V_{\alpha\beta}(x - y) \rho_{\alpha s}(x) \rho_{\beta s}(y), \quad (4)$$

where the integral kernel  $V_{\alpha\beta}(x - y) = 2\pi v_F \delta_{\alpha\beta} \delta(x - y) + U_{\alpha\beta}(x - y)$  includes both the kinetic energy of the free chiral electrons with Fermi velocity  $v_F$  as well as the Coulomb interaction between electrons with interaction potential  $U_{\alpha\beta}(x)$ . At low energies the characteristic length scales are much longer than the screening length of the Coulomb interaction. Therefore, one can further approximate the Coulomb potential

as short ranged, i.e.,  $U_{\alpha\beta}(x - y) = U_{\alpha\beta} \delta(x - y)$ , with nonzero diagonal and off-diagonal interaction strengths  $U_{\alpha\beta}$  [34].

The current cross correlations can be calculated by using the scattering approach locally at QPC3 [55]. One finds that the cross correlations of the outgoing currents after QPC3 at zero frequency are given by a sum of two terms [47,48],

$$S_{1u,1d}(\omega = 0) = \mathcal{P}_1(0) + \mathcal{P}_2(0). \quad (5)$$

The first term is associated with a transmitted noise and has the simple form

$$\mathcal{P}_1(0) = \frac{e^2 V}{2\pi \hbar} (1 - T) T \sum_{s=u,d} T_{1s} (1 - T_{1s}). \quad (6)$$

The second term describes the generated noise by QPC3,

$$\mathcal{P}_2(0) = 2(1 - T) T a^{-2} \int dt K_u(t) G_d(t), \quad (7)$$

where  $a$  is the short-distance cutoff from bosonization and

$$K_u(t) = \langle e^{-i\phi_{1u}(L,t)} e^{i\phi_{1u}(L,0)} \rangle, \\ G_d(t) = \langle e^{i\phi_{1d}(L,t)} e^{-i\phi_{1d}(L,0)} \rangle. \quad (8)$$

All bosonic fields should be evaluated at the position  $x = L$  of QPC3 and the averages in the correlation functions are taken with respect to the nonequilibrium state created by the source QPC1 and QPC2. Next, we apply the nonequilibrium bosonization technique [50,51,53] to evaluate these correlation functions.

The Hamiltonian of the edge states in Eq. (4) generates the equation of motion of the bosonic fields  $\phi_{\alpha s}(x, t)$ . The latter have to be supplemented with the appropriate boundary conditions due to source QPCs, resulting in

$$\partial_t \phi_{\alpha s}(x, t) = -\frac{1}{2\pi} \sum_{\beta} \int dy V_{\alpha\beta}(x - y) \partial_y \phi_{\beta s}(y, t), \\ \partial_t \phi_{\alpha s}(0, t) = -2\pi j_{\alpha s}^{\text{in}}(t), \quad (9)$$

where the incoming currents  $j_{\alpha s}^{\text{in}}(t)$  are defined at the point  $x = 0^+$  right after the source QPC1 and QPC2. These equations of motion can be solved by diagonalizing the interaction matrix  $V_{\alpha\beta} = 2\pi v_F \delta_{\alpha\beta} + U_{\alpha\beta}$  via a Bogoliubov rotation,  $V = S(\theta) \Lambda S^\dagger(\theta)$ , which conserves the commutation relations of the bosonic fields. The rotation angle is determined by the strength of the electron-electron interaction and is given by  $\tan(2\theta) = 2V_{12}/(V_{11} - V_{22})$ . The new collective excitations are characterized by two velocities,  $\Lambda = \text{diag}(u, v)$ , where  $u, v = (V_{11} + V_{22})/2 \pm \sqrt{(V_{11} - V_{22})^2/4 + V_{12}^2}$  and we used that  $V_{12} = V_{21}$ . Imposing the boundary conditions (9) we obtain the dynamics of bosonic fields in both channels  $s \in \{u, d\}$ ,

$$\phi_{1s}(x, t) = -\lambda_1 \mathcal{Q}_{1s}(t_u) - \lambda_2 \mathcal{Q}_{2s}(t_u) - \lambda'_1 \mathcal{Q}_{1s}(t_v) + \lambda_2 \mathcal{Q}_{2s}(t_v), \\ \lambda_1 = \pi[1 - \cos(2\theta)], \quad \lambda_2 = \pi \sin(2\theta), \\ \lambda'_1 = 2\pi - \lambda_1, \quad (10)$$

where we have introduced the injected charges

$$\mathcal{Q}_{\alpha s}(t) = \int_{-\infty}^t dt' j_{\alpha s}^{\text{in}}(t') \quad (11)$$

and the times  $t_u = t - x/u$  and  $t_v = t - x/v$ . Therefore, the bosonic fields (10) at observation point  $x$  at time  $t$  are determined by the charges which arrive with different delay times  $t_u$  and  $t_v$ , and these charges are weighted with coupling constants due to intra- and interchannel electron-electron interactions. Now we have all the necessary ingredients to calculate the generated noise from Eq. (7).

### III. GAUSSIAN NOISE REGIME

First, we consider the case of Gaussian fluctuations of the bosonic fields. This means that the correlation function in Eq. (8) can be written as  $\log K_u(t) = 2\pi \langle j_{1u}^{\text{in}} \rangle t + \langle \phi_{1u}(L, t) \phi_{1u}(L, 0) \rangle - \langle \phi_{1u}^2(L, t) \rangle / 2 - \langle \phi_{1u}^2(L, 0) \rangle / 2$ , where  $\langle j_{1u}^{\text{in}} \rangle = VT_{1u}/2\pi$  is the current injected from upper QPC1. Now using Eq. (10) we obtain

$$\begin{aligned} \log K_u(t) &= iT_{1u}Vt - \int \frac{d\omega}{\omega^2} (1 - e^{-i\omega t})(\mathcal{F}_1 + \mathcal{F}_2), \\ \mathcal{F}_1 &= 2\pi \left[ 1 - \frac{\lambda_1 \lambda'_1}{\pi^2} \sin^2 \left( \frac{\omega t_L}{2} \right) \right] S_{1u}^{\text{in}}(\omega), \\ \mathcal{F}_2 &= \frac{2\lambda_2^2}{\pi} \sin^2 \left( \frac{\omega t_L}{2} \right) S_{2u}^{\text{in}}(\omega), \end{aligned} \quad (12)$$

where we have introduced the spectral function of current fluctuations,  $S_{1u}^{\text{in}}(\omega) = \int dt e^{i\omega t} \langle \delta j_{1u}^{\text{in}}(t) \delta j_{1u}^{\text{in}}(0) \rangle$ , and the delay time between wave packets,  $t_L = L/v - L/u$ , where  $L$  is the distance between the injection QPCs and QPC3. A similar expression can be obtained for  $G_d(t)$  by replacing the subscript  $u$  with  $d$ .

To obtain the spectral function of the incoming state, we again use the free-fermion scattering approach [55] because the interactions do not influence the tunneling at the injection QPCs. The general result for  $\alpha \in \{1, 2\}$  and  $s \in \{u, d\}$  at zero temperature and finite bias is then given by the sum of two terms,

$$S_{\alpha s}^{\text{in}}(\omega) = S_q(\omega) + (1 - T_{\alpha s})T_{\alpha s}S_n(\omega), \quad (13)$$

where  $S_q(\omega) = \omega\theta(\omega)/2\pi$  is the equilibrium ground state contribution and  $S_n(\omega) = \sum_{\pm} S_q(\omega \pm V) - 2S_q(\omega)$  is the nonequilibrium part which originates from the voltage-biased injection QPCs. Substituting Eq. (12) into Eq. (7), the second term in Eq. (5) takes the following final form,

$$\mathcal{P}_2(0) = -\frac{e^2V}{2\pi\hbar} 2(1 - T)T \int \frac{dz}{2\pi} \frac{e^{i(T_{1u} - T_{1d})z}}{(z - i0^+)^2} K_n(z), \quad (14)$$

where we have introduced the dimensionless integration variable  $z = Vt$  and used

$$\begin{aligned} \log K_n(z) &= -2[(1 - T_{1u})T_{1u} + (1 - T_{1d})T_{1d}] \\ &\times \int_0^1 \frac{dx}{x^2} (1 - x)[1 - \cos(zx)] \\ &\times \left[ 1 - \frac{\lambda_1 \lambda'_1}{\pi^2} \sin^2 \left( \frac{xL}{2L_{\text{ex}}} \right) \right], \end{aligned} \quad (15)$$

where  $L_{\text{ex}} = uv/[(u - v)V]$  is the characteristic correlation length between the two modes with velocities  $u$  and  $v$  and  $x = \omega/V$  is the dimensionless variable of integration.

In order to understand and compare the case of Gaussian noise to experimental data, we consider the generalized Fano

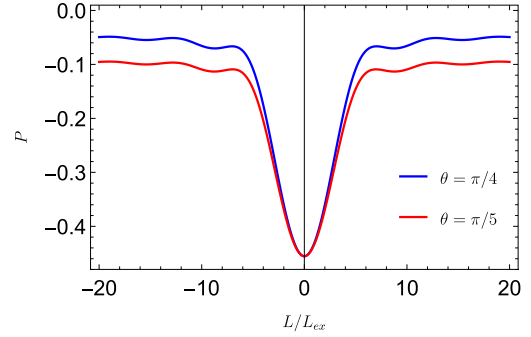


FIG. 2. The generalized Fano factor  $P$  as a function of the dimensionless length  $L/L_{\text{ex}}$  for different values of the interaction strength, parametrized by  $\lambda_1 = \pi[1 - \cos(2\theta)]$ , in the Gaussian noise regime. We set  $T_s = 0.15$ .

factor (2) at  $T_{1u} = T_{1d} =: T_s$ ,

$$\begin{aligned} P &= 1 - T_s + \frac{1}{T_s} \int \frac{dz}{2\pi} \frac{e^{-4R_s T_s \Phi(\lambda_1, L/L_{\text{ex}}, z)}}{(z - i0^+)^2}, \quad \Phi(\lambda_1, L/L_{\text{ex}}, z) \\ &= \int_0^1 \frac{dx}{x^2} (1 - x)[1 - \cos(zx)] \left[ 1 - \frac{\lambda_1 \lambda'_1}{\pi^2} \sin^2 \left( \frac{xL}{2L_{\text{ex}}} \right) \right], \end{aligned} \quad (16)$$

as a function of the dimensionless variable  $L/L_{\text{ex}}$ . Figure 2 shows that the Fano factor is negative, in contrast to experimental data from Ref. [47], indicating that the experiment was perhaps not performed in the Gaussian regime.

Finally, we would like to mention briefly that our results do not apply in the strictly noninteracting limit. In that case, the two modes have identical velocities,  $u = v$ , which leads to a divergence  $L_{\text{ex}} \rightarrow \infty$ .

### IV. NON-GAUSSIAN NOISE REGIME

Next, we consider the fluctuations of the bosonic fields as non-Gaussian at long distances  $L \gg L_{\text{ex}}/\min\{T_{1u}, T_{1d}\}$ . The physical situation we consider here corresponds to the case where the correlation function in Eq. (8) may be strongly affected by high-order boundary current cumulants from Eq. (9). In particular, such a situation arises in the case of strong interaction for  $\lambda_1 = \pm\pi$ . At such distances, the partitioned charges  $Q_{1s}$  at the source QPCs, taken at times  $t_u$  and  $t_v$ , can be considered as uncorrelated. Therefore, the correlation functions associated with the upper and lower parts of the collider in Eq. (8) split into products of four factors,

$$\begin{aligned} K_u(t) &= \chi_{1u}(\lambda_1, t) \chi_{1u}(\lambda'_1, t) \chi_{2u}(\lambda_2, t) \chi_{2u}(-\lambda_2, t), \\ G_d(t) &= \chi_{1d}(-\lambda_1, t) \chi_{1d}(-\lambda'_1, t) \chi_{2d}(-\lambda_2, t) \chi_{2d}(\lambda_2, t), \end{aligned} \quad (17)$$

where each factor represents a generator of full counting statistics (FCS) [34],

$$\chi_{\alpha s}(\lambda, t) = \langle e^{i\lambda Q_{\alpha s}(t)} e^{-i\lambda Q_{\alpha s}(0)} \rangle. \quad (18)$$

For the nonequilibrium state created at QPC1 and QPC2, the generating function can be written analytically in the long-time Markovian limit, which gives the main contribution to

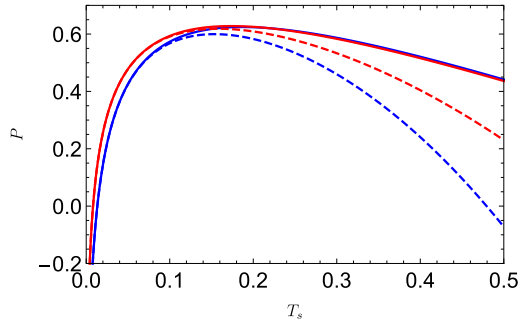


FIG. 3. The generalized Fano factor  $P$  as a function of source transparency  $T_s$  in the regime of non-Gaussian noise. The solid lines are numerical results based on Eq. (2) and the dashed lines are the asymptotics in Eq. (21). The blue and red curves correspond to  $\theta = \pi/4$  (strong interaction) and  $\theta = \pi/5$ .

integrals in Eq. (7). This is known as the Levitov-Lee-Lesovik formula [56]. In the Poissonian regime of small transparencies  $T_{1s} \ll 1$ , the Levitov-Lee-Lesovik formula at zero temperature for positive times  $t > 0$  is given by

$$\log \chi_{\alpha s}(\lambda, t) = \frac{\lambda^2}{4\pi^2} \log\left(\frac{\gamma}{it + \gamma}\right) - \frac{Vt}{2\pi} T_{\alpha s} (1 - e^{i\lambda}), \quad (19)$$

where  $\gamma \propto a/(2\pi v_F)$  is related to the short-distance cutoff  $a$ . For  $t < 0$  the FCS can be calculated by analytic continuation of Eq. (19), namely  $\chi_{\alpha s}(\lambda, -t) = \chi_{\alpha s}^*(\lambda, t)$ . Since the channels with subscript  $\alpha = 2$  are not biased and  $T_{2s} = 0$ , the FCS generators for these channels are given by the first term of Eq. (19). It is worth mentioning that this is the ground state (Fermi sea) contribution. However, the channels with  $\alpha = 1$  include the second term, which is a non-Gaussian contribution. Substituting the FCS generator (19) into Eqs. (17) and (7), the second term of the noise at  $T_{1u} = T_{1d} =: T_s$  turns out to be equal to

$$\mathcal{P}_2(0) = -\frac{e^2 V}{2\pi \hbar} \int \frac{dz}{2\pi} \frac{\exp[-2T_s f(\lambda_1) |z|/\pi]}{(z - i0^+)^2}, \quad (20)$$

where  $f(\lambda_1) = 1 - \cos(\lambda_1)$  and  $z = Vt$  is the dimensionless integration variable. Now, substituting Eq. (20) into Eq. (5) and then into Eq. (2), we get the final formula for the generalized Fano factor to leading order in the transparency of the injection QPCs,

$$P = 1 - T_s + \frac{2f(\lambda_1)}{\pi^2} [\mathcal{C} - \pi \tilde{T}_s - \log(1/\tilde{T}_s)], \quad (21)$$

where  $\mathcal{C} = \log 2 + \gamma$ ,  $\gamma \approx 0.5772$  is Euler's constant, and  $\tilde{T}_s = T_s f(\lambda_1)$  is the renormalized transparency of the source QPCs. Note that for  $\theta = \pi/4$ , which corresponds to strong electron-electron interactions, one finds  $f(\lambda_1) = 2$ . It is worth

mentioning that the subleading corrections in  $T_s$  show nonanalytical behavior as well and are proportional to  $\log(1/\tilde{T}_s^2)$ . The result (21) does not depend on length explicitly because the calculations were done in the limit of large  $L$ , when a complete separation of the wave packets with velocities  $u$  and  $v$  occurs. The generalized Fano factor as a function of source transparency  $T_s$  and for different interaction strengths  $\theta$  is plotted in Fig. 3.

## V. CONCLUSION

To summarize, we have studied the zero-frequency current cross correlations and the corresponding generalized Fano factor in a mesoscopic quantum Hall collider at filling factor  $\nu = 2$ . We have used nonequilibrium bosonization in order to take into account both the nonequilibrium state created by the source QPCs as well as the electron-electron interactions. We have shown that both the noise and the Fano factor consist of two terms. The first term is associated with the transmitted noise and is proportional to  $T_s(1 - T_s)$ . This term only contains information about the nonequilibrium conditions after the injection QPCs. The second term, which mixes the incoming nonequilibrium states, is related with the generated noise. It shows a nonanalytical dependence on the source transparency and scales as  $T_s \log(1/T_s)$  at small  $T_s \ll 1$  in case of strong, screened Coulomb interactions ( $\theta = \pi/4$ ). The nonanalytical behavior is robust with respect to the interaction parameter and does not vanish for  $\theta \neq \pi/4$ . Thus, the generated noise contains information both about the nonequilibrium state after the source QPCs and the electron-electron interactions. The same considerations are valid for the generalized Fano factor. It is known that the absence of current correlations for free fermions at filling factor  $\nu = 1$  is due to perfect spatial exclusion, while the negative correlations for Laughlin anyons at  $\nu = 1/3$  in the non-Gaussian noise regime are a signature of a reduced spatial exclusion [48]. However, for filling factor  $\nu = 2$  and experimentally accessible transparencies  $T_s \geq 0.05$  [47], we have shown that the Fano factor in the non-Gaussian regime of the injection QPCs is positive, in contrast to the cases for free fermions and Laughlin quasiparticles. The positive correlations arise due to the additional Coulomb interactions between fermions.

## ACKNOWLEDGMENTS

We are grateful to G. Fève for sharing experimental data and for fruitful discussions. E.G.I. and T.L.S. acknowledge financial support from the National Research Fund Luxembourg under Grant No. CORE C19/MS/13579612/HYBMES. E.V.S. acknowledges support from the Swiss National Science Foundation.

## APPENDIX A: GAUSSIAN NOISE REGIME

In this Appendix we derive the Eqs. (12) and (14) of the main text. In order to do this we use the Gaussian nature of the theory. This entails that

$$K_{ii}(t) = \langle e^{-i\phi_{1u}(t)} e^{i\phi_{1u}(0)} \rangle = e^{-i(\phi_{1u}(t) - \phi_{1u}(0))} e^{\langle \phi_{1u}(t)\phi_{1u}(0) \rangle - \langle \phi_{1u}^2(0) \rangle}. \quad (A1)$$

We first we calculate the phase. Using Eq. (10) of the main text and taking into account that the injection current is  $\langle j_{in,1u}(t') \rangle = VT_{1u}/2\pi$  and  $\lambda_1 + \lambda'_1 = 2\pi$ , we obtain

$$-i\langle \phi_{1u}(t) - \phi_{1u}(0) \rangle = i\lambda_1 \langle Q_{1u}(t - L/u) - Q_{1u}(-L/u) \rangle + i\lambda'_1 \langle Q_{1u}(t - L/v) - Q_{1u}(-L/v) \rangle = iT_{1u}Vt. \quad (A2)$$

Next, again using Eq. (10) and introducing the notation  $t_L = L/v - L/u$ , the remaining part in exponent has the form

$$\langle \phi_{1u}(t)\phi_{1u}(0) \rangle = \lambda_1\lambda'_1 \{ \langle Q_{1u}(t + t_L)Q_{1u}(0) \rangle + \langle Q_{1u}(t - t_L)Q_{1u}(0) \rangle - 2\langle Q_{1u}(t)Q_{1u}(0) \rangle \} + (2\pi)^2 \langle Q_{1u}(t)Q_{1u}(0) \rangle - \lambda_2^2 \{ \langle Q_{2u}(t + t_L)Q_{2u}(0) \rangle + \langle Q_{2u}(t - t_L)Q_{2u}(0) \rangle - 2\langle Q_{2u}(t)Q_{2u}(0) \rangle \}. \quad (A3)$$

Now, substituting the two-point correlation function of charge operators.

$$\langle Q_{1s}(t)Q_{1s}(0) \rangle = \int d\omega e^{-i\omega t} S_{1s}^{\text{in}}(\omega)/2\pi\omega^2, \quad S_{1s}^{\text{in}}(\omega) = \int dt e^{i\omega t} \langle \delta J_{1s}^{\text{in}}(t) \delta j_{1s}^{\text{in}}(0) \rangle, \quad (A4)$$

into Eq. (A3), we obtain the two-point correlation function for the bosonic fields

$$\langle \phi_{1u}(t)\phi_{1u}(0) \rangle = 2\pi \int \frac{d\omega e^{-i\omega t} S_{1u}^{\text{in}}(\omega)}{\omega^2} \left[ 1 - \frac{\lambda_1\lambda'_1}{\pi^2} \sin^2(\omega t_L/2) \right] + 2\pi \int \frac{d\omega e^{-i\omega t} S_{2u}^{\text{in}}(\omega)}{\omega^2} \left( \frac{\lambda}{\pi} \right)^2 \sin^2(\omega t_L/2). \quad (A5)$$

Furthermore, combining this with  $-\langle \phi_{1u}^2(0) \rangle$  and the phase factor  $iT_{1u}Vt$ , we get the following equation for the correlation function,

$$\log K_u(t) = iT_{1u}Vt - 2\pi \int \frac{d\omega}{\omega^2} (1 - e^{-i\omega t}) \left\{ \left[ 1 - \frac{\lambda_1\lambda'_1}{\pi^2} \sin^2\left(\frac{\omega t_L}{2}\right) \right] S_{1u}^{\text{in}}(\omega) + \left(\frac{\lambda_2}{\pi}\right)^2 \sin^2\left(\frac{\omega t_L}{2}\right) S_{2u}^{\text{in}}(\omega) \right\}. \quad (A6)$$

This is Eq. (12) of the main text. A similar expression can be obtained for  $G_d(t)$  with a minus sign in phase,

$$\log G_d(t) = -iT_{1d}Vt - 2\pi \int \frac{d\omega}{\omega^2} (1 - e^{-i\omega t}) \left\{ \left[ 1 - \frac{\lambda_1\lambda'_1}{\pi^2} \sin^2\left(\frac{\omega t_L}{2}\right) \right] S_{1d}^{\text{in}}(\omega) + \left(\frac{\lambda_2}{\pi}\right)^2 \sin^2\left(\frac{\omega t_L}{2}\right) S_{2d}^{\text{in}}(\omega) \right\}. \quad (A7)$$

In the case of zero temperature and a finite bias the fluctuations of the incoming currents  $S_{1s}^{\text{in}}(\omega)$  are given by [55]

$$S_{1s}^{\text{in}}(\omega) = S_q(\omega) + T_{1s}(1 - T_{1s}) \sum_{\pm} [S_q(\omega \pm V) - 2S_q(\omega)], \quad S_q(\omega) = \omega\theta(\omega)/2\pi. \quad (A8)$$

Substituting the correlation functions  $K_u(t)$  and  $G_d(t)$  into Eqs. (8), (7), and (2), and introducing the dimensionless integration variables  $x = \omega/V$  and  $z = Vt$ , we obtain Eqs. (14) and (16) of the main text.

## APPENDIX B: NON-GAUSSIAN NOISE REGIME

In this Appendix we derive Eq. (17) of the main text. Since we are interested in the regime of non-Gaussian noise we cannot simply use Eq. (A1) of the previous section. Instead, we use the fact that at long distances  $L \gg L_{\text{ex}}/\min\{T_{1u}, T_{1d}\}$ , the charges  $Q_{1s}(t)$  evaluated at different times  $t_u = t - L/u$  and  $t_v = t - L/v$  are uncorrelated. Consequently, the calculations are simplified as follows,

$$\begin{aligned} K_u(t) &= \langle e^{-i\phi_{1u}(t)} e^{i\phi_{1u}(t)} \rangle \\ &= \langle e^{i[\lambda_1 Q_{1u}(t_u) + \lambda_2 Q_{2u}(t_u) + \lambda'_1 Q_{1u}(t_v) - \lambda_2 Q_{2u}(t_v)]} e^{-i[\lambda_1 Q_{1u}(t_u - t) + \lambda_2 Q_{2u}(t_u - t) + \lambda'_1 Q_{1u}(t_v - t) - \lambda_2 Q_{2u}(t_v - t)]} \rangle \\ &= \langle e^{i[\lambda_1 Q_{1u}(t_u) + \lambda'_1 Q_{1u}(t_v)]} e^{-i[\lambda_1 Q_{1u}(t_u - t) + \lambda'_1 Q_{1u}(t_v - t)]} \rangle \langle e^{i[\lambda_2 Q_{2u}(t_u) - \lambda_2 Q_{2u}(t_v)]} e^{-i[\lambda_2 Q_{2u}(t_u - t) - \lambda_2 Q_{2u}(t_v - t)]} \rangle \\ &\simeq \langle e^{i\lambda_1 Q_{1u}(t_u)} e^{-i\lambda_1 Q_{1u}(t_u - t)} \rangle \langle e^{i\lambda'_1 Q_{1u}(t_v)} e^{-i\lambda'_1 Q_{1u}(t_v - t)} \rangle \langle e^{i\lambda_2 Q_{2u}(t_u)} e^{-i\lambda_2 Q_{2u}(t_u - t)} \rangle \langle e^{-i\lambda_2 Q_{2u}(t_v)} e^{i\lambda_2 Q_{2u}(t_v - t)} \rangle \\ &= \underbrace{\langle e^{i\lambda_1 Q_{1u}(t_u)} e^{-i\lambda_1 Q_{1u}(0)} \rangle}_{\chi_{1u}(\lambda_1, t)} \underbrace{\langle e^{i\lambda'_1 Q_{1u}(t_v)} e^{-i\lambda'_1 Q_{1u}(0)} \rangle}_{\chi_{1u}(\lambda'_1, t)} \underbrace{\langle e^{i\lambda_2 Q_{2u}(t_u)} e^{-i\lambda_2 Q_{2u}(0)} \rangle}_{\chi_{2u}(\lambda_2, t)} \underbrace{\langle e^{-i\lambda_2 Q_{2u}(t_v)} e^{i\lambda_2 Q_{2u}(0)} \rangle}_{\chi_{2u}(-\lambda_2, t)} \\ &= \chi_{1u}(\lambda_1, t) \chi_{1u}(\lambda'_1, t) \chi_{2u}(\lambda_2, t) \chi_{2u}(-\lambda_2, t). \end{aligned} \quad (B1)$$

Similarly, one can show that  $G_d(t) = \chi_{1d}(-\lambda_1, t) \chi_{1d}(-\lambda'_1, t) \chi_{2d}(-\lambda_2, t) \chi_{2d}(\lambda_2, t)$ . Therefore, we obtain Eq. (17) of the main text.

- [1] Z. F. Ezawa, *Quantum Hall Effects*, 3rd ed. (World Scientific, Singapore, 2013).  
 [2] D. C. Glattli, *The Quantum Hall Effect* (Birkhäuser, Basel, 2005), pp. 163–197.

- [3] E. Bocquillon, V. Freulon, F. D. Parmentier, J.-M. Berroir, B. Plaças, C. Wahl, J. Rech, T. Jonckheere, T. Martin, C. Grenier, D. Ferraro, P. Degiovanni, and G. Fève, *Ann. Phys.* **526**, 1 (2014).

- [4] B. Roussel, C. Cabart, G. Fève, E. Thibierge, and P. Degiovanni, *Phys. Status Solidi B* **254**, 1600621 (2017).
- [5] I. P. Levkivskiy and E. V. Sukhorukov, *Phys. Rev. B* **78**, 045322 (2008).
- [6] Y. Ji, Y. Chung, D. Sprinzak, M. Heiblum, D. Mahalu, and H. Shtrikman, *Nature (London)* **422**, 415 (2003).
- [7] I. Neder, M. Heiblum, Y. Levinson, D. Mahalu, and V. Umansky, *Phys. Rev. Lett.* **96**, 016804 (2006).
- [8] S. Tewari, P. Roulleau, C. Grenier, F. Portier, A. Cavanna, U. Gennser, D. Mailly, and P. Roche, *Phys. Rev. B* **93**, 035420 (2016).
- [9] H. Duprez, E. Sivre, A. Anthore, A. Aassime, A. Cavanna, U. Gennser, and F. Pierre, *Science* **366**, 1243 (2019).
- [10] A. A. Clerk, P. W. Brouwer, and V. Ambegaokar, *Phys. Rev. Lett.* **87**, 186801 (2001).
- [11] E. G. Idrisov, I. P. Levkivskiy, and E. V. Sukhorukov, *Phys. Rev. Lett.* **121**, 026802 (2018).
- [12] S. Jezouin, Z. Iftikhar, A. Anthore, F. D. Parmentier, U. Gennser, A. Cavanna, A. Ouerghi, I. P. Levkivskiy, E. Idrisov, E. V. Sukhorukov, L. I. Glazman, and F. Pierre, *Nature (London)* **536**, 58 (2016).
- [13] Z. Iftikhar, A. Anthore, A. K. Mitchell, F. D. Parmentier, U. Gennser, A. Ouerghi, A. Cavanna, C. Mora, P. Simon, and F. Pierre, *Science* **360**, 1315 (2018).
- [14] A. Furusaki and K. A. Matveev, *Phys. Rev. B* **52**, 16676 (1995).
- [15] E. G. Idrisov, I. P. Levkivskiy, and E. V. Sukhorukov, *Phys. Rev. B* **96**, 155408 (2017).
- [16] E. Sivre, A. Anthore, F. D. Parmentier, A. Cavanna, U. Gennser, A. Ouerghi, Y. Jin, and F. Pierre, *Nat. Phys.* **14**, 145 (2018).
- [17] M. Banerjee, M. Heiblum, A. Rosenblatt, Y. Oreg, D. E. Feldman, A. Stern, and V. Umansky, *Nature (London)* **545**, 75 (2017).
- [18] M. Banerjee, M. Heiblum, V. Umansky, D. E. Feldman, Y. Oreg, and A. Stern, *Nature (London)* **559**, 205 (2018).
- [19] C. Altimiras, H. le Sueur, U. Gennser, A. Cavanna, D. Mailly, and F. Pierre, *Nat. Phys.* **6**, 34 (2010).
- [20] H. le Sueur, C. Altimiras, U. Gennser, A. Cavanna, D. Mailly, and F. Pierre, *Phys. Rev. Lett.* **105**, 056803 (2010).
- [21] C. Altimiras, H. le Sueur, U. Gennser, A. Cavanna, D. Mailly, and F. Pierre, *Phys. Rev. Lett.* **105**, 226804 (2010).
- [22] D. L. Kovrizhin and J. T. Chalker, *Phys. Rev. Lett.* **109**, 106403 (2012).
- [23] I. P. Levkivskiy and E. V. Sukhorukov, *Phys. Rev. B* **85**, 075309 (2012).
- [24] A. O. Slobodeniuk, E. G. Idrisov, and E. V. Sukhorukov, *Phys. Rev. B* **93**, 035421 (2016).
- [25] K. Itoh, R. Nakazawa, T. Ota, M. Hashisaka, K. Muraki, and T. Fujisawa, *Phys. Rev. Lett.* **120**, 197701 (2018).
- [26] T. Krähenmann, S. G. Fischer, M. Roosli, T. Ihn, C. Reichl, W. Wegscheider, K. Ensslin, Y. Gefen, and Y. Meir, *Nat. Commun.* **10**, 3915 (2019).
- [27] E. G. Idrisov, I. P. Levkivskiy, and E. V. Sukhorukov, *Phys. Rev. B* **101**, 245426 (2020).
- [28] A. Rosenblatt, S. Konyzheva, F. Lafont, N. Schiller, J. Park, K. Snizhko, M. Heiblum, Y. Oreg, and V. Umansky, *Phys. Rev. Lett.* **125**, 256803 (2020).
- [29] B. J. van Wees, H. van Houten, C. W. J. Beenakker, J. G. Williamson, L. P. Kouwenhoven, D. van der Marel, and C. T. Foxon, *Phys. Rev. Lett.* **60**, 848 (1988).
- [30] D. C. Glattli and P. S. Roulleau, *Phys. Status Solidi B* **254**, 1600650 (2017).
- [31] C. Bäuerle, D. C. Glattli, T. Meunier, F. Portier, P. Roche, P. Roulleau, S. Takada, and X. Waintal, *Rep. Prog. Phys.* **81**, 056503 (2018).
- [32] G. Reborna, M. Acciai, D. Ferraro, and M. Sassetti, *Phys. Rev. B* **101**, 245310 (2020).
- [33] T. Morel, J.-Y. M. Lee, H.-S. Sim, and C. Mora, *Phys. Rev. B* **105**, 075433 (2022).
- [34] I. P. Levkivskiy, *Mesoscopic Quantum Hall Effect*, 1st ed. (Springer, Berlin, 2012).
- [35] X.-G. Wen, *Phys. Rev. B* **44**, 5708 (1991).
- [36] C. de C. Chamon, D. E. Freed, and X. G. Wen, *Phys. Rev. B* **51**, 2363 (1995).
- [37] C. de C. Chamon, D. E. Freed, and X. G. Wen, *Phys. Rev. B* **53**, 4033 (1996).
- [38] A. Crépieux, P. Devillard, and T. Martin, *Phys. Rev. B* **69**, 205302 (2004).
- [39] I. Safi, P. Devillard, and T. Martin, *Phys. Rev. Lett.* **86**, 4628 (2001).
- [40] A. M. Chang, *C. R. Phys.* **3**, 677 (2002).
- [41] C. L. Kane and M. P. A. Fisher, *Phys. Rev. Lett.* **72**, 724 (1994).
- [42] C. L. Kane and M. P. A. Fisher, *Phys. Rev. B* **67**, 045307 (2003).
- [43] G. Dolcetto, S. Barbarino, D. Ferraro, N. Magnoli, and M. Sassetti, *Phys. Rev. B* **85**, 195138 (2012).
- [44] J. Rech, D. Ferraro, T. Jonckheere, L. Vannucci, M. Sassetti, and T. Martin, *Phys. Rev. Lett.* **118**, 076801 (2017).
- [45] E. G. Idrisov, *Phys. Rev. B* **100**, 155422 (2019).
- [46] M. Kapfer, P. Roulleau, M. Santin, I. Farrer, D. A. Ritchie, and D. C. Glattli, *Science* **363**, 846 (2019).
- [47] H. Bartolomei, M. Kumar, R. Bisognin, A. Marguerite, J.-M. Berroir, E. Bocquillon, B. Plaçais, A. Cavanna, Q. Dong, U. Gennser, Y. Jin, and G. Fève, *Science* **368**, 173 (2020).
- [48] B. Rosenow, I. P. Levkivskiy, and B. I. Halperin, *Phys. Rev. Lett.* **116**, 156802 (2016).
- [49] J. Nakamura, S. Liang, G. C. Gardner, and M. J. Manfra, *Nat. Phys.* **16**, 931 (2020).
- [50] I. P. Levkivskiy and E. V. Sukhorukov, *Phys. Rev. Lett.* **103**, 036801 (2009).
- [51] I. P. Levkivskiy and E. V. Sukhorukov, *Phys. Rev. Lett.* **109**, 246806 (2012).
- [52] D. B. Gutman, Y. Gefen, and A. D. Mirlin, *Europhys. Lett.* **90**, 37003 (2010).
- [53] D. B. Gutman, Y. Gefen, and A. D. Mirlin, *Phys. Rev. B* **81**, 085436 (2010).
- [54] X.-G. Wen, *Adv. Phys.* **44**, 405 (1995).
- [55] Y. Blanter and M. Büttiker, *Phys. Rep.* **336**, 1 (2000).
- [56] L. S. Levitov, H. Lee, and G. B. Lesovik, *J. Math. Phys.* **37**, 4845 (1996).